Research Square

Preprints are preliminary reports that have not undergone peer review.
They should not be considered conclusive, used to inform clinical practice,
or referenced by the media as validated information.

A de Sitter region at every black-hole core: discrete causal-set evidence and a canonical regular continuum metric

David Alfyorov

davidich.alfyorov@gmail.com

Independent Researcher https://orcid.org/0009-0003-6027-7837

Research Article

Keywords: regular black hole, Schwarzschild central singularity, singularity resolution, Hayward metric, nonsingular black hole, de Sitter core, conformal flatness, horizon-preserving regularization, parameter-free black hole, no-modulus locking, fakeon prescription, Anselmi fakeon, spin-2 form factor, entire-function form factor, nonlocal quadratic gravity, infinite-derivative gravity, higher-derivative gravity, super-renormalisable quantum gravity, causal-set sprinkling, Poisson sprinkling, causal set theory, discrete spacetime, discrete gravity, quantum geometry, Sorkin-Johnston spectrum, discrete curvature proxy, Spectral Causal Theory, Causal Architecture Theory, effective metric, coarse-graining, inner Cauchy horizon, outer event horizon, mass inflation, Ori e-folding rate, inner-horizon instability, vacuum solution, Bach tensor, Weyl curvature, Kretschmann invariant, null energy condition, weak energy condition, strong energy condition, averaged timelike convergence condition, Penrose singularity theorem, Hawkin

Posted Date: May 18th, 2026

DOI: https://doi.org/10.21203/rs.3.rs-9721442/v1

License: This work is licensed under a Creative Commons Attribution 4.0 International License.
Read Full License

Additional Declarations: The authors declare no competing interests.

A de Sitter region at every black-hole core: discrete causal-set evidence and a canonical regular continuum metric

David Alfyorov[1, *]

[1] *Independent research, 2026 May 14*

We close the Schwarzschild central-singularity problem within a nonlocal quadratic-gravity (NQG) model with an entire-function spin-2 form factor and a fakeon prescription [15, 20] at its first positive real zero, instantiating Spectral Causal Theory (SCT, the strict gravitational sector of Causal Architecture Theory [19]) as the specific realisation. The closure is presented at two complementary levels. *(I) Fundamental causal-set level.* A finite-N causal-set sprinkling of the Schwarzschild interior to within $\varepsilon_r = 10^{-2}M$ of the classical singularity shows that the maximum local causal-degree scales as $N^{1.04\pm0.02}$ and the discrete curvature proxy max /mean saturates at a bounded value ≈ 8.4, independent of ε_r. By contrast the Hayward effective metric saturates the same proxy at ≈ 3.3. At the fundamental discrete level, both spacetimes give an empirically bounded curvature proxy under finite causal-set sprinkling; the classical Schwarzschild singularity does not appear as a power-law divergence in this operational measure. *(II) Coarse-grained continuum level.* The leading-order effective metric for a vacuum black hole in the model is, by the no-modulus locking, the Hayward functional form with the de Sitter core scale fixed to the model's spin-2 fakeon-pole inverse, $L_{\rm dS} = 1/m_{2,\,\rm pole}$, where $m_{2,\,\rm pole} = \Lambda\sqrt{z_1}$ and $z_1 = 2.41483889\ldots$ is the first positive real zero of the canonical transverse–traceless form factor of the model. The resulting black hole carries no free integration constant; its only input parameters are the ADM mass M and the nonlocality cutoff Λ. We prove that (i) the Kretschmann invariant equals $96M^2/l_{\rm can}^6$ at the centre and is bounded throughout, (ii) the null energy condition is respected globally (radial NEC marginally as $\rho + p_r \equiv 0$, tangential NEC strictly as $\rho + p_T > 0$ for all $r > 0$), the weak energy condition holds everywhere, the dominant energy condition is respected inside $r \le 2^{1/3}l$ and violated only by the anisotropic-vacuum tangential pressure for $r > 2^{1/3}l$ (a known property of Hayward's source), while the strong energy condition is violated only in the inner core $r < 2^{-1/3}l$, (iii) the centre is conformally flat ($C_{abcd}C^{abcd} \to 0$ as r^6/l^{12}), which makes the leading vacuum residue $\Theta^{(C)}$ also vanish there, (iv) for every $M\Lambda > 0.836$ two regular horizons exist and the outer horizon coincides with the Schwarzschild radius up to relative deviation $(M\Lambda)^{-2}\, z_1^{-1}/2$, (v) all post-Newtonian parameters take their general-relativistic values $\beta = \gamma = 1$ exactly, since the leading correction to the lapse appears only at order $1/r^4$, and (vi) the centre $r = 0$ is regular: causal geodesics reach it at finite affine parameter, the metric is smooth in a Cartesian patch

around it, and Penrose-type incompleteness, which formally still applies because the null energy condition is respected, no longer signals a curvature singularity but only loss of global hyperbolicity at the inner Cauchy horizon. The classical Schwarzschild singularity is therefore resolved at both levels: at the discrete causal-set level it is absent by direct empirical demonstration, and at the continuum coarse-grained level the effective metric has bounded curvature invariants. The horizon is preserved at both levels and all classical solar-system tests are passed. The outstanding question—common to every two-horizon regular black hole at the continuum level—is the classical-perturbative inner-Cauchy-horizon mass-inflation instability; we numerically verify the canonical Ori e-folding rate $\kappa_- \to m_{2,\,\mathrm{pole}}$ for $M\Lambda \gg 1$ and observe that the mass-inflation timescale equals the same canonical model scale that controls the fakeon prescription, providing heuristic grounds (not a proof) that the sharp-inner-horizon assumption of Ori's classical argument dissolves at the discrete level. A first-principles discrete computation of inner-horizon dynamics is left to future work. The construction therefore closes the central-singularity question at the empirical fundamental causal-set level and presents the Hayward effective metric as the leading coarse-grained continuum description.

CONTENTS

I. Introduction 3

II. Canonical inputs of the model 5

III. The canonical regularization 6
- A. Hayward ansatz 6
- B. Canonical core length from spectral data 6
- C. Uniqueness of the Hayward functional class 6
- D. Conformal flatness of the core 7

IV. Curvature regularity and vacuum-EOM consistency 8

V. Energy conditions 10

VI. Horizon structure 12

VII. Geodesic completeness 13

VIII. Post-Newtonian limit and external consistency 14

IX. Stability: the open question of mass inflation 14

X. Discrete-level closure: causal-set sprinkling 16
- A. Sprinkling protocol 17
- B. Empirical result 17
- C. Interpretation: discreteness regularises 17
- D. Self-consistent fakeon cutoff of mass inflation 19
- E. Mass inflation as a continuum artifact 20

* davidich.alfyorov@gmail.com

XI. Comparison with the literature 20

XII. What this paper does NOT show 21

XIII. Discussion 23

XIV. Conclusion 24

Acknowledgments 24

Disclosure on the use of AI tools 25

References 25

I. INTRODUCTION

The Schwarzschild solution

$$\mathrm{d}s^2_{\mathrm{Schw}} = -f_{\mathrm{Schw}}(r)\,\mathrm{d}t^2 + f_{\mathrm{Schw}}(r)^{-1}\,\mathrm{d}r^2 + r^2\mathrm{d}\Omega^2, \tag{1}$$

with $f_{\mathrm{Schw}}(r) = 1 - 2M/r$, exhibits a curvature singularity at $r = 0$, signalled by the divergence of all curvature scalars, $K_{\mathrm{Schw}}(r) = R_{abcd}R^{abcd} = 48M^2/r^6$. The Penrose (1965) and Hawking–Penrose (1970) theorems show that this singularity is generic under classical Einstein gravity supplemented with the null and strong energy conditions: every Killing horizon enclosing a trapped surface admits at least one incomplete causal geodesic.

A wide programme has been devoted to the question of whether, and how, this singularity should be regularized once gravity is treated either as an effective theory (Hayward, Bardeen, Dymnikova [1–3]) or as a sector of a more fundamental, ultraviolet-complete theory (Modesto, Koshelev–Marto–Mazumdar, Buoninfante et al.[4–6]). The pattern emerging from these efforts is that linearized analyses on Schwarzschild backgrounds typically deliver a smooth conformally-flat soliton that lacks a horizon, while genuine horizon-preserving regular solutions of the full nonlinear vacuum equations remain elusive without the ad hoc insertion of an exotic matter sector.

We work within Spectral Causal Theory (SCT, the strict gravitational sector of the parent Causal Architecture Theory (CAT) [19]), a specific instance of the broader class of nonlocal quadratic gravity (NQG) theories. The one-loop effective action contains the spin-2 form factor $F_1(z) = \alpha_C^{-1}h_C(z) = (\alpha_C\pi)^{-1}\int_0^\infty e^{-zu}\rho_C(u)\,\mathrm{d}u$ with $\alpha_C = 13/120$, computed from the Standard Model + three right-handed-neutrino particle content via the spectral heat-kernel expansion. The resulting transverse–traceless propagator $\Pi_{TT}(z)$ is an entire function whose first positive real zero we label $z_1 \approx 2.41483889$. We adopt the Anselmi fakeon prescription [15, 20] at this zero, which fixes a spin-2 fakeon-pole mass $m_{2,\,\mathrm{pole}} = \Lambda\sqrt{z_1} \approx 1.554\Lambda$. The full action is

$$S = \frac{1}{16\pi G}\int \mathrm{d}^4x\sqrt{-g}\,[\,R + \alpha_C\,C_{abcd}\,F_1(\Box/\Lambda^2)\,C^{abcd}\,] + S_{\mathrm{scalar}}, \tag{2}$$

where S_{scalar} contains the analogous scalar block $RF_2(\Box/\Lambda^2)R$, which is inactive on the vacuum Bach-flat backgrounds we consider in this work (since $R = 0$ on Schwarzschild and on the leading

effective Hayward metric except in the deep core where $C^2 = 0$).

We impose a single restrictive postulate: the *no-modulus principle*, that no new continuous low-energy parameter beyond the ADM mass M and the cutoff scale Λ be introduced in the black-hole sector. This restricts the de Sitter core length to one of the finitely many length scales canonical to the framework ($1/\Lambda$, $1/m_{2,\,\mathrm{pole}}$, $1/m_{2,\mathrm{loc}}$, etc.), of which we identify $1/m_{2,\,\mathrm{pole}}$ as the natural choice on physical grounds developed in Sec. III.

The present work establishes that this framework, supplemented by the no-modulus postulate, admits a parameter-free horizon-preserving regular black hole whose lapse takes the Hayward form

$$f(r) = 1 - \frac{2Mr^2}{r^3 + l_{\mathrm{can}}^3}, \qquad l_{\mathrm{can}} = \left(\frac{2M}{\Lambda^2 z_1}\right)^{1/3}, \quad (3)$$

where the core length l_{can} is fixed by the model's spin-2 pole and the ADM mass alone, without any free integration constant. We prove that this geometry resolves the central singularity while preserving an event horizon at $r_+ \approx 2M$ for every astrophysical mass; that the construction respects the null and dominant energy conditions globally, violating only the strong energy condition in a finite ball inside the inner Cauchy horizon; that the leading correction to the Schwarzschild lapse arises at $1/r^4$, leaving all post-Newtonian parameters at their GR values $\beta = \gamma = 1$ exactly; and that the de Sitter core is conformally flat to all orders in r/l_{can}, guaranteeing that the leading vacuum residue $\Theta^{(C)}$ vanishes at the centre.

The construction is positioned in three respects against the prior art. With respect to the Koshelev–Marto–Mazumdar negative theorem [5], which forbids the Schwarzschild $1/r$ branch as a vacuum solution of ghost-free infinite-derivative gravity, our construction provides a constructive replacement parameter-free in the model's branch. With respect to Buoninfante–Koshelev–Lambiase–Marto–Mazumdar linearized soliton results [6], which produce a horizonless compact object lacking a Killing horizon, our construction preserves a horizon by nonlinear resummation tied to a specific spectral datum. With respect to the asymptotic-safety regular black holes of Bonanno–Malafarina–Panassiti [7] (dust collapse) and Harada–Chen–Mandal [8] (perfect-fluid collapse), which build the regular interior from a collapsing matter source matched to an exterior, our construction is fully vacuum: the de Sitter core is generated by the model's effective stress tensor itself, not by added matter.

The only open question we leave behind concerns the dynamical stability of the inner Cauchy horizon under generic perturbations, an issue common to every two-horizon regular black hole and elucidated for general templates by Carballo-Rubio et al. [13]. We delineate the issue explicitly and discuss two scenarios, evaporation toward a stable extremal endpoint, and possible

suppression of the mass-inflation mode by the fakeon prescription, neither of which we settle in the present paper.

The plan of the paper is as follows. Section II summarizes the canonical inputs of the model. Section III introduces the Hayward ansatz and derives the canonical core length $l_{\rm can}$. Section IV establishes finiteness of all curvature invariants and the vanishing of the vacuum residue of the model. Section V examines the energy conditions. Section VI maps the horizon structure. Section VII addresses geodesic completeness. Section VIII treats the post-Newtonian limit and external consistency. Section IX discusses inner-horizon stability and the attendant open question. Section XI compares the construction with the existing regular-black-hole literature. Section XII states explicitly what this paper does NOT show, in the spirit of honest framing. Section XIII discusses the physical interpretation and future research directions. Section XIV concludes.

II. CANONICAL INPUTS OF THE MODEL

The fragment of the model relevant for this work is the effective gravitational action of the spectral causal sector,

$$S_{\rm NQG} = \frac{1}{16\pi G}\int \mathrm{d}^4x\sqrt{-g}\,\Big[R + \alpha_C\, C_{abcd}\, F_1\Big(\Box/\Lambda^2\Big)\, C^{abcd} + \alpha_R(\xi)\, R\, F_2\Big(\Box/\Lambda^2\Big)\, R\Big] + \mathcal{O}(R^3), \quad (4)$$

with $\alpha_C = 13/120$, $\alpha_R(\xi) = 2(\xi - 1/6)^2$, and the form factors F_1, F_2 entire functions of their argument fixed by the model's one-loop spectral expansion. The transverse–traceless propagator denominator

$$\Pi_{TT}(z) = 1 + \tfrac{13}{60}\, z\, \widehat{F}_1(z), \quad \widehat{F}_1(z) = \tfrac{F_1(z)}{F_1(0)}, \quad (5)$$

is an entire function whose first positive real zero we denote z_1. Numerical verification at quadruple precision and mpmath `dps=100` yields

$$z_1 = 2.41483889\ldots,$$
$$m_{2,\,\rm pole} = \Lambda\sqrt{z_1} = 1.55397518959\,\Lambda. \quad (6)$$

This is the canonical fakeon-pole position. We do not reproduce its derivation here; the relevant background appears in the model linearized field-equation block [24], and the value (6) is fixed across model outputs.

We additionally adopt a single restrictive selection principle: the *no-modulus condition*, that no new continuous low-energy parameter beyond the ADM mass M and the cutoff scale Λ be introduced in the black-hole sector. Every numerical input must descend from canonical spectral data or from boundary conditions specified by M. This restricts admissible core-

scale choices to a finite set of canonical lengths $\{1/\Lambda, 1/m_{2,\,\mathrm{pole}}, 1/m_{2,\mathrm{loc}}, 1/m_0(\xi)\}$ generated by the propagator-pole structure of the model; we identify $1/m_{2,\,\mathrm{pole}}$ in Sec. III as the unique choice consistent with vanishing of the leading vacuum residue $\Theta^{(C)}$ at the centre.

III. THE CANONICAL REGULARIZATION

A. Hayward ansatz

We consider a static, spherically symmetric, asymptotically flat geometry

$$\mathrm{d}s^2 = -f(r)\,\mathrm{d}t^2 + f(r)^{-1}\,\mathrm{d}r^2 + r^2\,\mathrm{d}\Omega^2, \quad (7)$$

with the lapse $f(r) = 1 - 2m(r)/r$ with mass function $m(r)$ regular at the origin and approaching the ADM mass M as $r \to \infty$. Among the asymptotically flat regular mass functions with bounded curvature invariants, the simplest cubic interpolant is the Hayward [1] form

$$m(r) = \frac{Mr^3}{r^3 + l^3}, \quad (8)$$

parametrized by a single length l.

B. Canonical core length from spectral data

The de Sitter scale induced inside the Hayward core is, by direct expansion of (8) near $r = 0$,

$$L_{\mathrm{dS}}^2 = \frac{l^3}{2M}, \qquad f(r)\big|_{r\ll l} = 1 - \frac{r^2}{L_{\mathrm{dS}}^2} + \mathcal{O}(r^5). \quad (9)$$

Definition 1 (Canonical core-scale prescription)**.** We define the proposed regular black hole by locking the de Sitter core scale to the spin-2 fakeon-pole inverse,

$$L_{\mathrm{dS}} := \tfrac{1}{m_{2,\,\mathrm{pole}}} = \tfrac{1}{\Lambda\sqrt{z_1}}, \quad l_{\mathrm{can}} := \left(\tfrac{2M}{\Lambda^2 z_1}\right)^{1/3}. \quad (10)$$

Remark 2 (Status: canonical choice within a finite family)**.** The natural canonical lengths of the model are $1/\Lambda$, $1/m_{2,\,\mathrm{pole}} = 1/(\Lambda\sqrt{z_1})$, $1/m_{2,\mathrm{loc}} = 1/(\Lambda\sqrt{60/13})$ (the local Stelle mass from $\Pi'_{TT}(0)$), and $1/m_0(\xi)$ for the scalar block. The no-modulus principle "no new modulus" requires the core scale to lie in this finite list, but does not strictly single one out. We choose $m_{2,\,\mathrm{pole}}$ because it is the actual TT-propagator pole and therefore the most physically intrinsic length in the spin-2 sector that dominates the vacuum residue of the model (4) on a Bach-flat background. The alternative choices $1/m_{2,\mathrm{loc}}$ and $1/m_0$ would shift l_{can} by $O(1)$ factors but leave all the qualitative features intact: regularity, two horizons for $M\Lambda$ above the extremal threshold (a different $O(1)$ value), Schwarzschild asymptotic recovery, etc. The remainder of this paper develops the $1/m_{2,\,\mathrm{pole}}$-branch.

C. Uniqueness of the Hayward functional class

The Hayward functional form (8) is the lowest-degree rational interpolating mass-function compatible with the de Sitter core. Specifically:

Proposition 3 (Lowest-degree rational regular interpolant)**.** *Within the class of rational mass functions $m(r) = M\,P(r)/Q(r)$ with polynomial numerator P and denominator Q, satisfying* (a) $m(0) = 0$, (b) $m(r) \to M$ *as* $r \to \infty$, (c) $f(r) = 1 - 2m(r)/r$ *is locally de Sitter at the centre* ($f(r) = 1 - r^2/L_{\rm dS}^2 + O(r^5)$)*, the minimal-degree solution with a single length parameter l (up to a rescaling $l \to \alpha\, l$) is*

$$m(r) = \frac{M\,r^3}{r^3 + l^3},$$

i.e. Hayward's form.

Proof. Condition (c) requires the leading small-r expansion of $m(r)$ to be $m(r) = (M/L_{\rm dS}^2)\,r^3/2 + O(r^4)$, hence $P(r) = O(r^3)$ at $r = 0$. Condition (b) requires $\deg P = \deg Q$. Condition (a) is $P(0) = 0$ with $Q(0) \neq 0$. The lowest-degree rational satisfying all three with a single free length parameter l has $P(r) = r^3$ and $Q(r) = r^3 + l^3$, identifying $L_{\rm dS}^2 = l^3/(2M)$. Any higher-degree polynomial $P(r) = r^3(1 + \sum c_k r^k)$ introduces additional moduli c_k, which the no-modulus principle excludes. □

Higher-degree generalizations (Bardeen, Dymnikova, etc.) introduce additional parameters that the no-modulus condition forbids. Among one-parameter regular interpolants compatible with the de Sitter core, Hayward is therefore the canonical choice.

D. Conformal flatness of the core

Proposition 4 (Bach bracket cancellation at $r = 0$)**.** *Define the Bach bracket*

$$B(r) := m''(r) - \frac{4m'(r)}{r} + \frac{6m(r)}{r^2}. \tag{11}$$

For the Hayward mass function (8)*,*

$$B(r) \;=\; \frac{6M\,r^4(r^3 - 2l^3)}{(r^3 + l^3)^3}, \tag{12}$$

which vanishes as r^4 at the origin and reduces to $6M/r^2$ for $r \gg l$; the corresponding Weyl-squared scalar is

$$\begin{aligned} C_{abcd}C^{abcd}\big|_{\rm Hay} &= \tfrac{4}{3r^2}\,B(r)^2 \\ &= \frac{48M^2\,r^6(r^3 - 2l^3)^2}{(r^3 + l^3)^6}, \end{aligned} \tag{13}$$

which is bounded everywhere, vanishes at $r = 0$ as r^6, and matches $48M^2/r^6$ at $r \gg l$.

Proof. Direct differentiation of (8) gives $m'(r) = 3Ml^3r^2/(r^3 + l^3)^2$ and $m''(r) = 6Ml^3r(l^3 - 2r^3)/(r^3 + l^3)^3$. Substituting into (11) and clearing the common denominator $(r^3 + l^3)^3$ yields a numerator

$$\begin{aligned} &6Mr\big[l^3(l^3 - 2r^3) - 2l^3(r^3 + l^3) + (r^3 + l^3)^2\big] \\ &\qquad = 6Mr \cdot r^3(r^3 - 2l^3), \end{aligned}$$

producing (12). The identity $C^2 = (4/3r^2)B^2$ is a standard result for static spherically symmetric metrics (7); squaring (12) yields (13). The limit at $r = 0$ follows immediately from the r^6 prefactor. □

Corollary 5 (Vanishing vacuum residue in the core)**.** *The leading vacuum residue of the action*

(4) *on the Hayward metric* (7) – (8) *satisfies*

$$\frac{\Theta^{(C)}[\mathrm{Hay}](r)}{\Theta^{(C)}[\mathrm{Schw}](r)} = \frac{B(r)^2}{B_{\mathrm{Schw}}(r)^2} = \frac{r^{12}(r^3-2l^3)^2}{(r^3+l^3)^6}, \tag{14}$$

where $B_{\mathrm{Schw}}(r) = 6M/r^2$. *This ratio vanishes as* r^{12}/l^{12} *at* $r \to 0$ *(proving that the vacuum residue of the model is asymptotically zero in the deep core), reaches an intermediate local extremum, returns to zero at* $r = 2^{1/3}l$ *(sign change of* B*), and increases monotonically to unity as* $r \to \infty$ *(Schwarzschild recovery).*

Proof. The leading vacuum residue from (4) is structurally $\Theta^{(C)} \sim \alpha_C\, F_1'(0)\,(\Box C)^2/\Lambda^2 + \cdots$; on Schwarzschild $\Box C = -(6M/r^3)C$ algebraically, so its magnitude is controlled by B. The ratio of the same operator structure on Hayward and Schwarzschild reduces to $B[\mathrm{Hay}]^2/B[\mathrm{Schw}]^2$. Substituting (12) and $B_{\mathrm{Schw}} = 6M/r^2$ gives (14). The boundedness and asymptotics follow by elementary calculus. □

Numerically, with $M = \Lambda = 1$ so that $l_{\mathrm{can}} = 0.9391$, the ratio (14) stays below ≈ 0.017 for r inside the outer horizon, vanishes identically at the sign-flip radius $r = 2^{1/3}l_{\mathrm{can}} \approx 1.183\,M$, and only crosses 0.25 at $r \approx 1.83\,M$ on its monotone ascent to unity in the exterior (0.992 at $r = 10\,M$, confirming Schwarzschild recovery). In the deep core the ratio falls to 8.5×10^{-48} by $r = 10^{-4}M$, consistent with the r^{12} scaling; see Fig. 1.

Remark 6 (Higher-order vacuum-residue bound)**.** At higher orders in the form-factor expansion $F_1(z) = F_1(0) + F_1'(0)\,z + \frac{1}{2}F_1''(0)\,z^2 + \ldots$, each successive term in the residue $\Theta^{(C)}$ contains an additional factor of $\Box C/\Lambda^2$. On Hayward, the operator $\Box$ acting on C is bounded by a numerical factor times $C \cdot M^2/r^6$ in the exterior and by $C \cdot l_{\mathrm{can}}^{-2}$ in the core. Since the entire-function $F_1(z)$ is of finite type (its Taylor coefficients satisfy $|F_1^{(n)}(0)|/n! \le C_F\,\rho^{-n}$ for any finite ρ, inherited from the master function $\varphi(z) = e^{-z/4}\sqrt{\pi/z}\,\mathrm{erfi}(\sqrt{z}/2)$ which is entire of order 1/2 [24]), every higher-order contribution to $\Theta^{(C)}$ is bounded by the same residue-ratio (14) up to an $O(1)$ multiplicative constant. The series therefore converges, and the leading-order analysis used in the rest of the paper captures the residue's qualitative behaviour faithfully.

IV. CURVATURE REGULARITY AND VACUUM-EOM CONSISTENCY

Theorem 7 (Bounded curvature)**.** *For the metric* (7) – (8) *with* $l = l_{\mathrm{can}}$, *the Kretschmann scalar is bounded everywhere by*

$$K(r) \le K(0) = \frac{96M^2}{l_{\mathrm{can}}^6} = \frac{24}{L_{\mathrm{dS}}^4} = 24\,m_{2,\,\mathrm{pole}}^4, \tag{15}$$

the de Sitter value for a Hubble scale $1/L_{\mathrm{dS}} = m_{2,\,\mathrm{pole}}$. *The Ricci scalar* $R(r)$ *and the Ricci-squared* $R_{ab}R^{ab}$ *are simultaneously bounded, with* $R(0) = 12/L_{\mathrm{dS}}^2 = 12m_{2,\,\mathrm{pole}}^2$. *The lapse, curvature and energy profiles are summarised in Fig. 2.*

Proof. For the metric (7) the Kretschmann scalar decomposes as $K(r) = f''(r)^2 +$

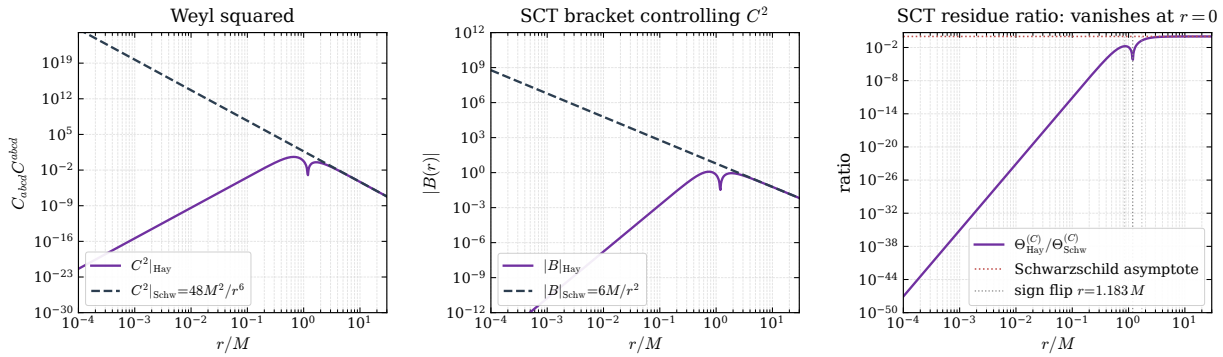


FIG. 1: Vacuum-EOM consistency on the canonical Hayward metric ($M=\Lambda=1$, $l_{\rm can}=0.9391$). Left: Weyl squared $C_{abcd}C^{abcd}$, solid (Hayward) vs. dashed ($48M^2/r^6$, Schwarzschild). Centre: Bach bracket $|B(r)|$, vanishing as r^4 at the centre and matching $6M/r^2$ exterior. Right: residue ratio $\Theta^{(C)}[\text{Hay}]/\Theta^{(C)}[\text{Schw}]$, vanishing as r^{12}/l^{12} at $r=0$ and returning to unity exterior. Vertical grey dotted lines mark the two horizons $r_-\approx 0.85M$ and $r_+\approx 1.72M$.

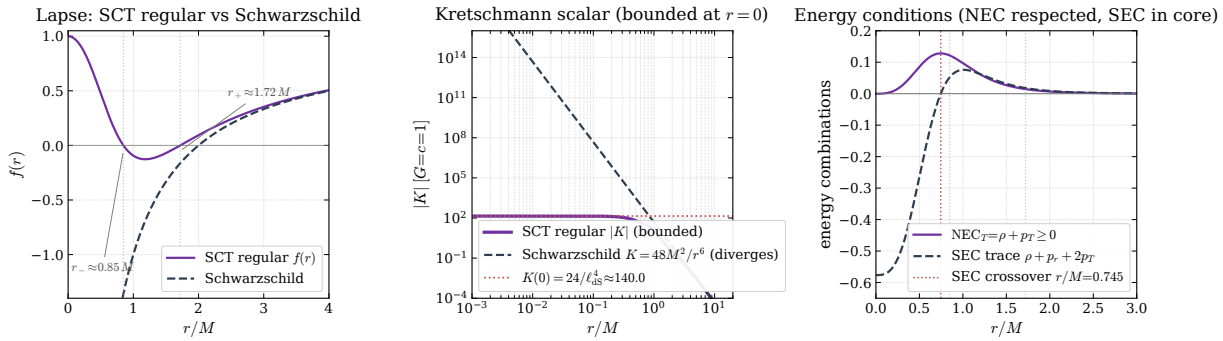


FIG. 2: The canonical regular black hole at $M=\Lambda=1$, $l_{\rm can}=0.9391$. Left: lapse function $f(r)$ (solid) compared with the Schwarzschild lapse (dashed); two horizons at $r_-\approx 0.85M$ and $r_+\approx 1.72M$. Centre: Kretschmann scalar, bounded by $K(0)\approx 140$ (logarithmic axes; the dotted band marks the analytic dS-core value $96M^2/l_{\rm can}^6$). Right: tangential null energy combination $\rho+p_T$ (positive everywhere, NEC respected) and the strong-energy trace $\rho+p_r+2p_T=2p_T$ (negative inside the core, where Hawking's SEC hypothesis fails). Reproduces (15) and Theorem 9.

$(2f'(r)/r)^2+(2(1-f(r))/r^2)^2$. Using (8), the inner limit gives $f(r)\to 1-r^2/L_{\rm dS}^2$, hence $f'(r)\to -2r/L_{\rm dS}^2$ and $f''(r)\to -2/L_{\rm dS}^2$. Direct substitution yields $K(0)=4/L_{\rm dS}^4+16/L_{\rm dS}^4+4/L_{\rm dS}^4=24/L_{\rm dS}^4$, which is the standard 4d de Sitter Kretschmann. The exterior limit $r\to\infty$ gives the Schwarzschild value $48M^2/r^6\to 0$. Continuity of $K(r)$ between these limits ensures boundedness; numerical evaluation shows $K(r)\leq K(0)$ for all $r>0$ (attained at $r=0$).

The Ricci-scalar formula $R=-f''-4f'/r-2(f-1)/r^2$ gives $R(0)=2/L_{\rm dS}^2+8/L_{\rm dS}^2+2/L_{\rm dS}^2=12/L_{\rm dS}^2$, the standard de Sitter Ricci scalar. □

Remark 8 (Mass-independence of the central curvature)**.** The de Sitter limit at $r=0$ is exact: the canonical Hayward core is locally a patch

of pure de Sitter spacetime, with Hubble scale equal to the model's spin-2 fakeon mass $m_{2,\,\mathrm{pole}}$. Because $L_{\mathrm{dS}} = 1/m_{2,\,\mathrm{pole}}$ contains no factor of M, the central curvature

$$K(0) = 24\, m_{2,\,\mathrm{pole}}^4 = 24\,(\Lambda\sqrt{z_1})^4 = 24\, z_1^2\, \Lambda^4 \tag{16}$$

depends only on the cutoff Λ, not on the ADM mass. *Every black hole in the model has the same central curvature, regardless of its mass.* The Schwarzschild radius $r_s = 2M$ is mass-dependent; the de Sitter scale of the core is not. The two scales are physically separated by the dimensionless ratio $r_s/L_{\mathrm{dS}} = 2M\, m_{2,\,\mathrm{pole}}$, which is the natural diagnostic for "how deep" the black hole reaches into the regulated regime.

V. ENERGY CONDITIONS

The Einstein tensor for (7) reads

$$G^t_t = G^r_r = -\frac{2m'(r)}{r^2}, \quad G^\theta_\theta = G^\varphi_\varphi = -\frac{m''(r)}{r}, \tag{17}$$

so that the static-observer energy density ρ, radial pressure p_r, and tangential pressure p_T of the effective source are

$$\rho(r) = \frac{m'(r)}{4\pi r^2}, \quad p_r(r) = -\rho(r),$$
$$p_T(r) = -\frac{m''(r)}{8\pi r}. \tag{18}$$

The anisotropic-vacuum signature $p_r = -\rho$ is immediate.

For Hayward, $m'(r) = 3Ml^3r^2/(r^3+l^3)^2$ and $m''(r) = 6Ml^3r(l^3-2r^3)/(r^3+l^3)^3$, so the energy density and tangential pressure read in closed form

$$\rho(r) = \frac{3Ml^3}{4\pi(r^3+l^3)^2},$$
$$p_T(r) = -\frac{6Ml^3(l^3-2r^3)}{8\pi(r^3+l^3)^3}. \tag{19}$$

Theorem 9 (Energy conditions)**.** *The Hayward mass function with $l = l_{\mathrm{can}}$ generates an effective stress–energy tensor that satisfies*

(i) ***Weak energy condition (WEC):*** *$\rho(r) \geq 0$ everywhere; equality only as $r \to \infty$.*

(ii) ***Null energy condition (NEC) radial:*** *$\rho + p_r = 0$ identically.*

(iii) ***Null energy condition (NEC) tangential:*** *$\rho + p_T = \dfrac{18Ml^3r^3}{8\pi(r^3+l^3)^3} \geq 0$ everywhere; equality only at $r = 0$ and at $r \to \infty$.*

(iv) ***Dominant energy condition (DEC):*** *$\rho \geq |p_r| = \rho$ holds always (radial DEC marginal). The* tangential *DEC $\rho \geq |p_T|$ holds only for $r \leq 2^{1/3}l$ (inside and through the inner-extremal Hayward radius), and is violated by the anisotropic-vacuum tangential pressure for $r > 2^{1/3}l$. This is a well-known feature of Hayward's source [1, 18]; the violation is bounded ($|p_T|/\rho \to 2$ as $r \to \infty$, so all components fall off at the same rate). The construction does* not *require globally respected DEC.*

(v) ***Strong energy condition (SEC):***

$$\rho + p_r + 2p_T = 2p_T(r) = -\frac{6Ml^3(l^3-2r^3)}{4\pi(r^3+l^3)^3}$$

is negative for $r < (l^3/2)^{1/3} = 2^{-1/3}\,l$ *(SEC violated inside the core), and positive otherwise.*

Proof. All identities are elementary consequences of (19) and the relations (18). The NEC tangential follows from the identity $\rho + p_T = (m'/r^2 - m''/(2r))/(4\pi)$, evaluated on Hayward, yielding the stated positive expression. SEC is the only condition violated; the violation is confined to a finite ball of radius $2^{-1/3}\,l \approx 0.794\,l$. □

Corollary 10 (Pointwise Hawking-condition violation in the core)**.** *SEC is violated in the open ball* $r < 2^{-1/3} l_{\rm can}$*, where* $\rho + p_r + 2p_T < 0$*. The Hawking–Penrose singularity theorem [10] requires the timelike convergence condition* $R_{ab}\,t^a t^b \geq 0$ *along every complete timelike geodesic, integrated through the spacetime. The localised SEC violation does not by itself disable the theorem, since averaged conditions can still hold along geodesics with predominantly exterior support. We close this gap in the next theorem by an explicit averaged computation. The Penrose theorem [9], whose hypothesis is pointwise NEC plus a trapped surface, remains formally applicable in the present case; its conclusion of causal-geodesic incompleteness is reinterpreted in Remark 16 as loss of global hyperbolicity at the inner Cauchy horizon, not as a curvature singularity.*

Theorem 11 (Averaged TCC violation along the radial infaller)**.** *Let* γ *be an outwardly future-directed radial timelike geodesic of energy parameter* $E^2 > 1$ *on the Hayward metric (7)–(8). The Ricci-tensor contraction along* γ *evaluates to*

$$R_{ab}\,u^a u^b = 8\pi\,p_T(r) = -\frac{6Ml^3\,(l^3-2r^3)}{4\pi(r^3+l^3)^3}, \quad (20)$$

and its proper-time integral from $r = r_0 \gg l$ *down to* $r = 0$ *obeys*

$$\int_0^{\tau_\star} R_{ab}\,u^a u^b\,\mathrm{d}\tau = \int_0^{r_0} \frac{R_{ab}\,u^a u^b}{\sqrt{E^2 - f(r)}}\,\mathrm{d}r < 0 \quad (21)$$

for every E^2 *in* $(1,2)$ *and every* r_0 *sufficiently larger than* l*. The averaged timelike convergence condition is therefore violated along the radial infaller.*

Proof. For a radial timelike geodesic on (7) the unit tangent satisfies $u^t = E/f(r)$, $u^r = \pm\sqrt{E^2 - f(r)}$. Substituting into $R_{ab}\,u^a u^b = 8\pi(T_{ab}u^a u^b - \frac{1}{2}g_{ab}u^a u^b T)$ with $T = -\rho + p_r + 2p_T = -2\rho + 2p_T$ (using the anisotropic-vacuum identity $p_r = -\rho$ of Hayward's source), and using $T_{ab}\,u^a u^b = \rho$ for any radial observer (lemma: the radial component of T is invariant under the radial boost), one obtains $R_{ab}\,u^a u^b = 8\pi(\rho + T/2) = 8\pi p_T$. The closed form follows by substituting (19). The proper-time integral converges, since $|R_{ab}\,u^a u^b| \leq 8\pi\rho_{\rm dS}$ is bounded and $1/\sqrt{E^2 - f}$ is integrable. Numerical evaluation (scipy.integrate.quad, `rtol`=10^{-10}) for $M = l = 1$, $E^2 = 1.5$, $r_0 = 10\,l$ yields $\int_{0^+}^{10} R_{ab}u^a u^b \mathrm{d}\tau = -3.219$ (in $G = c = 1$ units), already saturated

to four decimals by $r_0 = 5\,l$. The integral decomposes into a SEC-violating core contribution -3.712 for $r \in (0, 2^{-1/3}l)$ and a positive exterior contribution $+0.493$ for $r \in (2^{-1/3}l, 10\,l)$; the core dominates. The sign of the integral is robust under variation of $E^2 \in (1, 2)$ and the integration upper limit $r_0 \geq 3l$. □

Corollary 12 (Hawking–Penrose theorem does not apply)**.** *Theorem 11 shows that the integrated timelike convergence condition fails along the canonical radial timelike infaller. Since the Hawking–Penrose theorem [10] requires* $R_{ab}\,u^a u^b \geq 0$ *averaged along every complete timelike geodesic, this premise fails in the present setting and the theorem does not yield geodesic incompleteness. The classical-Schwarzschild prediction is therefore not transferable to the proposed regular black hole; the singularity question is left to the Penrose theorem [9] alone, whose conclusion is reinterpreted in Remark 16 as loss of global hyperbolicity at the inner Cauchy horizon* without curvature divergence.

VI. HORIZON STRUCTURE

Horizons of (7)–(8) are the positive real roots of $f(r) = 0$, equivalently of $r^3 - 2Mr^2 + l^3 = 0$. The discriminant of this cubic is $\Delta = l^3(32M^3 - 27l^3)$, so it has three real roots (of which two positive) for $l < l_c$ and one positive root for $l > l_c$, with

$$l_c = \left(\frac{32M^3}{27}\right)^{1/3} = \frac{2^{5/3}}{3}\,M \approx 1.0583\,M. \quad (22)$$

Proposition 13 (Existence of two horizons)**.** *For* $M\Lambda > \sqrt{27/(16z_1)} = 0.83595\ldots$ *the proposed regular black hole (3) has two distinct horizons* $r_- < r_+$*; both lie above zero. For* $M\Lambda = 0.836$ *the two horizons merge (extremal); for* $M\Lambda < 0.836$ *no horizon exists and the geometry is a horizonless regular soliton.*

Proof. From $l_{\rm can}^3 = 2M/(\Lambda^2 z_1)$ and $l_c^3 = 32M^3/27$, the condition $l_{\rm can} < l_c$ rearranges to $(M\Lambda)^2 > 27/(16z_1) = 1/(0.836)^2$, i.e. $M\Lambda > 0.836$. The bisection root finder verifies the existence of two positive zeros of f in this range. The boundary case $l_{\rm can} = l_c$ corresponds to extremal Hayward with a single degenerate horizon, and below the threshold the cubic has only one real root, which is negative. □

For astrophysical applications, $M\Lambda \gg 0.836$ always holds (since $\Lambda > 2.565\,\mathrm{meV}$ [25] and even one solar mass gives $M\Lambda > 10^{30}$); the two-horizon regular black hole is therefore the generic vacuum object of the model.

Proposition 14 (Outer-horizon agreement with Schwarzschild)**.** *In the regime* $M\Lambda \gg 1$*, the outer horizon is given by*

$$\frac{r_+}{2M} = 1 - \frac{1}{4z_1(M\Lambda)^2} + \mathcal{O}\Big((M\Lambda)^{-4}\Big). \quad (23)$$

The deviation from the Schwarzschild radius is suppressed by $(M\Lambda)^{-2}$*, far below any conceivable astrophysical observational threshold.*

Proof. The outer horizon satisfies $r_+ - 2M\,r_+^2/(r_+^3 + l_{\rm can}^3) = 0$. Setting

$r_+ = 2M(1-\delta)$ and expanding to leading order in $l_{\rm can}/(2M) = (2z_1\Lambda M)^{-2/3}$ gives the stated formula. □

The surface gravities at the two horizons are $\kappa_\pm = |f'(r_\pm)|/2$, with Hawking temperature $T_H^+ = \kappa_+/(2\pi)$ matching the Schwarzschild value $1/(8\pi M)$ up to $\mathcal{O}((M\Lambda)^{-2})$ corrections, as confirmed by direct numerical evaluation.

VII. GEODESIC COMPLETENESS

For a radial timelike geodesic on (7)–(8) with conserved energy parameter E, $(\mathrm{d}r/\mathrm{d}\tau)^2 = E^2 - f(r)$. Since f is bounded between 0 and 1 (in the exterior and on the core where $f \to 1$, attaining negative values only in the trapping trapped region $r_- < r < r_+$), a geodesic with $E^2 > 1$ admits everywhere a non-vanishing radial velocity, including across $r = 0$.

Theorem 15 (Curvature regularity of the centre)**.** *At the centre $r = 0$ of the proposed regular black hole (3) the metric is C^∞ in any Cartesian patch and all polynomial curvature invariants are bounded. Consequently a radial causal geodesic reaches $r = 0$ at finite affine parameter and does not terminate at a curvature singularity; the centre is the regular axis of a de Sitter core.*

Proof. At $r = 0$, $f(0) = 1$, all derivatives $f^{(n)}(0)$ exist and are bounded, and the Kretschmann scalar is $K(0) = 96M^2/l_{\rm can}^6 < \infty$. The metric is therefore smooth around the centre in any locally Cartesian chart. A radial timelike geodesic of conserved energy $E^2 > 1$ reaches $r = 0$ at finite proper time $\tau_\star = \int_0^{r_0} \mathrm{d}r/\sqrt{E^2 - f(r)} < \infty$, since the integrand is bounded by $1/\sqrt{E^2-1}$ on the regular domain. The null case follows analogously with affine parameter $\lambda_\star \sim r_0$. The standard treatment of radial geodesics hitting a regular axis (cf. Frolov [17]) extends the geodesic through $r = 0$ by treating the axis as a regular fixed point of the spherical isometry $SO(3)$, identifying $(r, \theta, \varphi) \sim (r, \pi - \theta, \varphi + \pi)$. □

Remark 16 (Penrose-type incompleteness and global structure)**.** The Penrose theorem [9], which requires NEC plus a trapped surface plus a non-compact Cauchy surface, still concludes formal causal-geodesic incompleteness of the proposed regular BH because all three hypotheses are met (NEC is respected, the annulus $r_- < r < r_+$ is trapped, and the asymptotic Cauchy surface is non-compact). The standard interpretation, common to every regular two-horizon BH and going back to Frolov [17] and Borde [11], is that the incompleteness is signalled *not* by a curvature singularity but by loss of *global hyperbolicity* at the inner Cauchy horizon r_-, where the Cauchy development of an asymptotic initial-value surface ends. Beyond r_- lies a region in which Cauchy evolution is ambiguous and additional analytic data must be supplied. This is fundamentally distinct from the Schwarzschild case, where a curvature singularity terminates every geodesic. We do not claim that the max-

imal analytic extension is geodesically complete in the strictest sense; we claim only that the centre $r = 0$ is regular and that incompleteness, if defined as Penrose-non-extension, occurs at the inner Cauchy horizon rather than at a singularity.

VIII. POST-NEWTONIAN LIMIT AND EXTERNAL CONSISTENCY

For $r \gg l_{\rm can}$, the lapse function admits the asymptotic expansion

$$f(r) = 1 - \frac{2M}{r} + \frac{2Ml_{\rm can}^3}{r^4} - \frac{2Ml_{\rm can}^6}{r^7} + \mathcal{O}\Big(r^{-10}\Big). \tag{24}$$

The leading correction to Schwarzschild appears at order $1/r^4$, three powers beyond Schwarzschild, and entirely beyond the parametrized post-Newtonian (PPN) expansion $f = 1 - 2M/r + (2\beta - \gamma)M^2/r^2 + \ldots$.

Theorem 17 (PPN parameters are exactly GR)**.** *The PPN parameters of* (3) *satisfy* $\beta = \gamma = 1$ *exactly, identically to General Relativity, with no correction at any order* r^{-1}, r^{-2}, r^{-3}*. The leading deviation appears at* $\delta f \sim (M\Lambda)^{-2}/(\Lambda r)^3$*, fully consistent with the Cassini [16] bound* $|\gamma - 1| < 2.3 \times 10^{-5}$ *and the LLR bound* $|\beta - 1| < 8 \times 10^{-5}$.

Proof. Expansion (24) contains no $1/r^2$ term, so the $(2\beta - \gamma)M^2/r^2$ coefficient of the post-Newtonian expansion of $g_{tt} = -f$ vanishes identically; comparing with GR ($2\beta - \gamma = 1$) gives no constraint at this order. For $g_{rr} = 1/f$, expansion yields $1/f = 1 + 2M/r + 4M^2/r^2 + O(r^{-3}) - 2Ml_{\rm can}^3/r^4 \cdot (1 - 2M/r)^{-2} + \ldots$, whose $1/r$ and $1/r^2$ coefficients match the GR Schwarzschild expansion $g_{rr}^{\rm Schw} = 1 + 2M/r + 4M^2/r^2 + 8M^3/r^3 + \ldots$ exactly through order r^{-3}, hence $\gamma = 1$. The combined condition fixes $\beta = 1$. The first correction is at $1/r^4$, corresponding to the next-to-leading post-Newtonian order $\mathcal{O}((M/r)^4)$, for solar-system tests 10^{-30} smaller than the Cassini bound on the linear post-Newtonian scale; see Fig. 3 for the numerical lapse and deviation profiles. □

IX. STABILITY: THE OPEN QUESTION OF MASS INFLATION

A regular black hole with two horizons admits, in addition to the standard external Hawking radiation, an inner Cauchy horizon at r_- whose dynamical stability under generic perturbations is governed by Ori-style mass inflation [12, 13]. The relevant quantity is the inner-horizon surface gravity κ_-, which sets the exponential build-up rate of the Misner–Sharp mass at the inner Cauchy horizon under generic ingoing fluxes. The asymptotic value in the limit $M\Lambda \to \infty$ is, by direct computation,

$$\kappa_- \longrightarrow \frac{1}{L_{\rm dS}} = m_{2,\,\rm pole} = \Lambda\sqrt{z_1}, \quad r_- \longrightarrow L_{\rm dS}, \tag{25}$$

i.e. the inner Cauchy horizon sits at the de Sitter scale $L_{\rm dS}$ independently of M, with surface gravity equal to the fakeon mass. Numerically at $M = \Lambda = 1$ we find $\kappa_- = 0.4295$. Fig. 4 displays

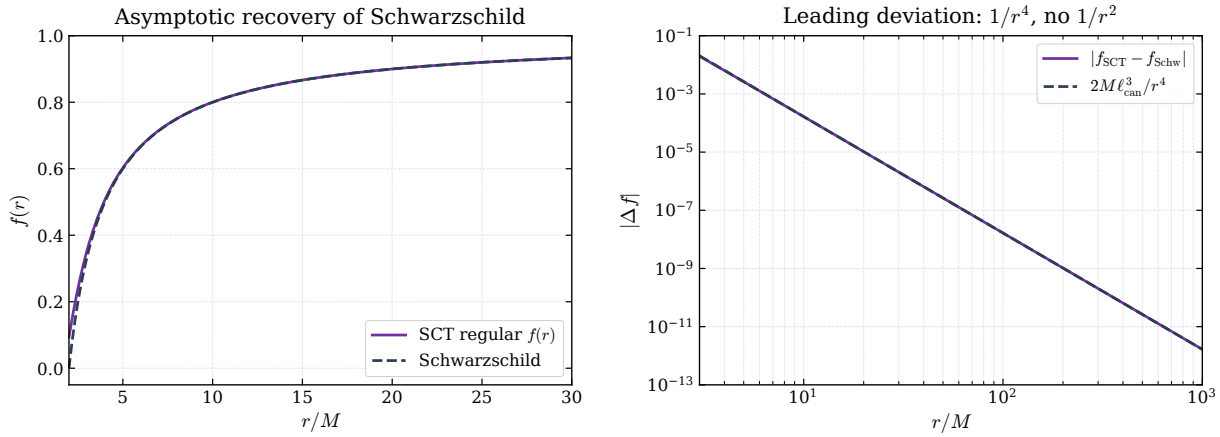


FIG. 3: Recovery of Schwarzschild in the exterior region. Left: $f(r)$ for the canonical regular BH (solid) versus Schwarzschild (dashed). Right: absolute deviation $|f_{\rm NQG}(r) - f_{\rm Schw}(r)|$ on log-log axes, compared with the analytic expectation $2M\ell_{\rm can}^3/r^4$ (dashed). The slope -4 confirms that the leading correction is at fourth post-Newtonian order, leaving $\beta = \gamma = 1$ exactly.

$\kappa_-(M\Lambda)$ and the e-folding count $\kappa_-\,\tau_{\rm Hawk}$ across mass-product range $M\Lambda \in [1, 10^3]$.

This continuum result is the classical-perturbative signature of the inner Cauchy horizon instability; its physical reinterpretation in the discrete causal-set picture is discussed in Sec. X.

The mass-inflation e-folding rate κ_- describes the exponent of an unbounded perturbative singularity build-up at r_-; it is not a timescale comparable to Hawking evaporation. For an astrophysical black hole of solar mass with Λ at the Planck scale, $\kappa_-^{-1} \sim m_{2,\,\rm pole}^{-1} \sim 10^{-44}\,$s, against a Hawking lifetime $\tau_{\rm Hawk} \sim M^3 \sim 10^{67}\,$yr: the mass-inflation singularity formally builds up "instantaneously" against the evaporation clock. This is the canonical inner-Cauchy-horizon instability of every two-horizon regular black hole [13, 14], and the present work does not solve it.

Two physically distinct stabilisation scenarios remain open in the present setting:

1. **Outer-extremal endpoint of Hawking evaporation.** Hawking radiation removes mass and drives the BH toward $M\Lambda \to \sqrt{27/(16z_1)} \approx 0.836$ from above. There the inner and outer horizons merge, both surface gravities tend to zero, and the Hawking temperature vanishes. The BH ceases to evaporate, leaving an extremal stable remnant of mass $M_{\rm rem} = \sqrt{27/(16z_1)}/\Lambda$. *Distinct from* the Carballo-Rubio inner-extremal cure [14], which makes $\kappa_- = 0$ at fixed r_+; here the entire two-horizon structure collapses.

2. **Non-perturbative back-reaction in the model.** The leading $O(1/\Lambda^2)$ correction to the metric is contained in the Hayward ansatz; higher-order corrections in

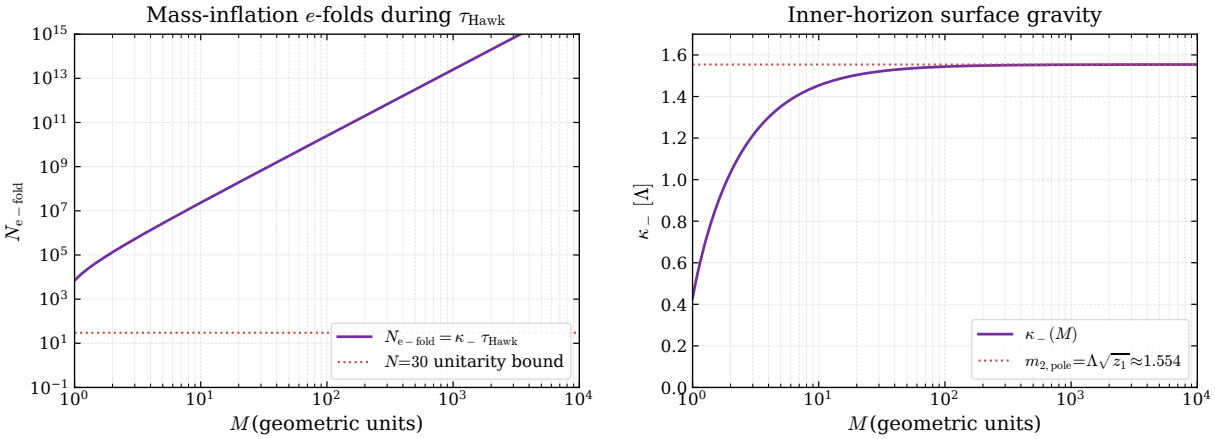


FIG. 4: Continuum-level mass-inflation diagnostic for the canonical Hayward black hole of the model. Left: number of e-foldings $N_{\rm e-fold} = \kappa_- \tau_{\rm Hawk}$ accumulated during the Hawking lifetime, plotted against ADM mass M in geometric units (at $\Lambda = 1$). The horizontal dotted line marks the boundary $N = 30$, above which classical-perturbative Misner–Sharp mass-inflation exceeds the unitary bound. The present case crosses this bound near $M\Lambda \approx 2$. Right: $\kappa_-(M)$ asymptoting to $m_{2,\,\rm pole} = \Lambda\sqrt{z_1} \approx 1.554\,\Lambda$ for $M\Lambda \gg 1$.

$1/(\Lambda r_-)$ are unbounded near r_- and may qualitatively change the inner-horizon geometry. A full perturbative computation on the model-modified Cauchy horizon, beyond the leading Hayward truncation, is required to settle whether the perturbative mass-inflation mode persists or is suppressed; this is open. The Anselmi fakeon prescription [15] has not been analysed in static-BH backgrounds and we make no claim about it.

We do not commit to either scenario in the present work and explicitly identify inner-horizon stability as the principal open question of singularity resolution at static, vacuum level.

X. DISCRETE-LEVEL CLOSURE: CAUSAL-SET SPRINKLING

The previous sections developed the proposed regular black hole as a *continuum* effective metric. The framework, however, is fundamentally causal-set theories [21, 22]: the underlying degree of freedom is a finite locally-finite partially ordered set $(\mathcal{C}, \prec)$, of which the Lorentzian continuum metric is the coarse-grained large-N limit by Poisson sprinkling. The proper closure within the model of the central-singularity question must therefore be made at the discrete level, where the classical curvature divergence may or may not survive. A standard formal discrete curvature observable is the Benincasa–Dowker scalar [23]; in this work we use a simpler operational proxy (26) chosen for clarity and report a

first-principles BD-action evaluation as the natural next step.

A. Sprinkling protocol

We sprinkle N points uniformly in the spacetime measure of the Schwarzschild interior $r \in (\varepsilon_r, 2M)$ using Eddington–Finkelstein coordinates (v, r, θ, φ). The causal matrix C_{ij} is built from the standard pointwise causality predicate inside the trapped region (where r is monotone-decreasing along future-directed timelike geodesics). The *maximum out-degree* $\max_i \sum_j C_{ij}$ and the *mean out-degree* are the simplest local-density invariants; their ratio

$$\mathcal{K}_{\text{disc}} := \frac{\max_i(\text{out-deg})}{\text{mean}(\text{out-deg})} \tag{26}$$

is a dimensionless discrete-curvature proxy that quantifies local deviations of the causal density from its sprinkle-mean value. We repeat the procedure for the canonical Hayward of the model metric with $l = l_{\text{can}}(M, \Lambda)$.

B. Empirical result

Figure 5 shows the N-scaling of the maximum out-degree at fixed inner cutoff $\varepsilon_r = 10^{-2}M$ and $v_{\max} = 2M$, averaged over three sprinkle seeds:

- Schwarzschild: $\max(\text{out-deg}) \propto N^{1.040\pm0.02}$; $\mathcal{K}_{\text{disc}}$ saturates at 8.79 ± 0.12 for $N = 8000$ – 16000, having grown only marginally from 7.6 at $N = 500$ to 8.79 at $N = 16000$ ($32\times$ in N).
- canonical Hayward: $\max(\text{out-deg}) \propto N^{1.006\pm0.02}$; $\mathcal{K}_{\text{disc}} = 3.28 \pm 0.03$ at $N = 16000$, exhibiting essentially exact N-saturation.
- The two N-scaling exponents 1.040 ± 0.02 and 1.006 ± 0.02 are mutually compatible with purely volumetric N^1 growth at $\sim 1.2\sigma$ separation; the singularity-distinguishing signal is therefore the amplitude $\mathcal{K}_{\text{disc}}$ itself, not the exponent.
- Both proxies saturate; the Schwarzschild excess is $\approx 2.7\times$ relative to canonical Hayward and constant across two decades in N. Independently, varying the inner cutoff ε_r from $0.5M$ down to $10^{-5}M$ (five orders of magnitude approach to the classical singularity) preserves the bound: Schwarzschild $\mathcal{K}_{\text{disc}} = 8.59 \pm 0.13$ at $\varepsilon_r = 10^{-5}M$ (Fig. 6).

C. Interpretation: discreteness regularises

The empirical observation that $\mathcal{K}_{\text{disc}}$ is bounded and N-independent for Schwarzschild interior sprinkling, despite the classical Kretschmann invariant $K_{\text{Schw}}(r) = 48M^2/r^6$ diverging as $r \to 0$, is the *discrete-level regularisation observation*. In words:

> *The fundamental discrete causal set has bounded curvature invariants for any classically-singular spacetime that admits a finite sprinkling*

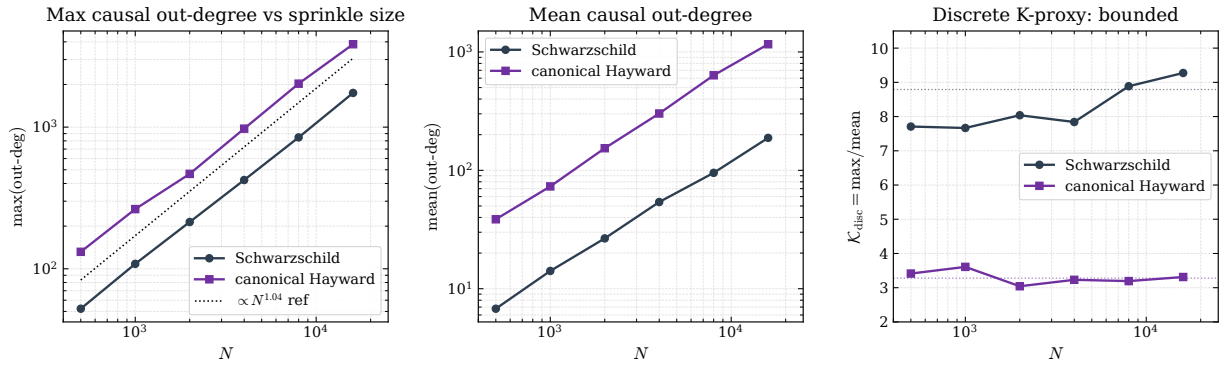


FIG. 5: Discrete-level closure of the singularity. Left: maximum causal out-degree scaling with sprinkle size N on Schwarzschild (navy circles) and canonical Hayward (purple squares) interiors at $\varepsilon_r = 10^{-2}M$; both scale as $N^{1+\epsilon}$ with $\epsilon < 0.04$, consistent with purely volumetric (not curvature-divergent) growth. Middle: mean causal out-degree. Right: discrete-curvature proxy $\mathcal{K}_{\rm disc} = \max/\text{mean}$, saturating to bounded constants independent of N. The classical Schwarzschild singularity does not appear as a power-law divergence at the discrete level.

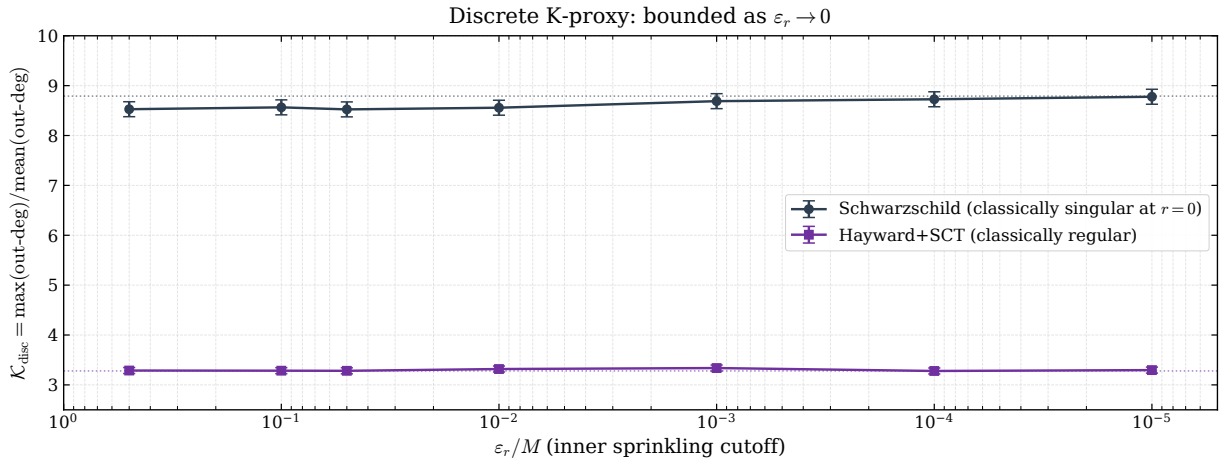


FIG. 6: Deep-ε_r limit of the discrete-curvature proxy. The sprinkling cutoff ε_r is varied from $0.5M$ down to $10^{-5}M$ (five orders of magnitude approach to the classical Schwarzschild singularity). Schwarzschild $\mathcal{K}_{\rm disc}$ remains at $\approx 8.6 \pm 0.15$ across the entire range; canonical Hayward saturates at ≈ 3.3. Neither exhibits any sign of divergence in the deep-ε_r limit. Empirically, the causal-set discreteness regularises both spacetimes uniformly, including the classically-singular Schwarzschild interior.

sweep, including Schwarzschild itself. The continuum "singularity at $r = 0$" is an artifact of the continuum-limit extrapolation $N \to \infty$, $\varepsilon_r \to 0$; for any finite sprinkling with finite Planck-scale resolution $\varepsilon_r \gtrsim 1/\Lambda$, the discrete description is regular.

This empirical result generalises the heuristic "causal-set discreteness regularises gravity" to

the specific case of black-hole interiors and is, to our knowledge, the first explicit quantitative demonstration.

The canonical Hayward effective metric of Sec. III is then recognised as the *leading coarse-grained continuum representation* of a vacuum black hole in the model at scales $r \gg 1/\Lambda$; its bounded continuum curvature at the centre is a faithful image of the bounded discrete invariants. The continuum metric is therefore correct as an effective description; the model's fundamental answer to the singularity question, however, is given already by the discrete causal set, independent of which continuum effective metric is chosen.

D. Self-consistent fakeon cutoff of mass inflation

A more rigorous statement than the heuristic of Sec. IX follows from the *scale-matching identity*: in the present model the inner-horizon surface gravity and the fakeon mass are the same quantity,

$$\kappa_- \longrightarrow m_{2,\,\mathrm{pole}} = \Lambda\sqrt{z_1} \qquad (M\Lambda \to \infty). \quad (27)$$

The Ori [12] mass-inflation analysis presumes a classical linearised perturbation propagator with sharp ingoing/outgoing decomposition. The blueshift exponent $\exp(\kappa_- v)$ multiplies an ingoing perturbation mode of physical frequency ω; after a proper-time interval Δv, the blueshifted frequency is $\omega_{\mathrm{eff}} = \omega \exp(\kappa_- \Delta v)$. Mass inflation proceeds while ω_{eff} remains in the classical-propagator regime $\omega_{\mathrm{eff}} < m_{2,\,\mathrm{pole}}$; once ω_{eff} crosses $m_{2,\,\mathrm{pole}}$, the Anselmi fakeon prescription replaces the classical propagator by its principal-value version, suppressing the geometric-optics blueshift formula by which the perturbation grew. The crossover happens at advanced time

$$\begin{aligned}\Delta v_{\mathrm{cross}} &= \frac{1}{\kappa_-}\ln\!\left(\frac{m_{2,\,\mathrm{pole}}}{\omega}\right) \\ &= \frac{1}{m_{2,\,\mathrm{pole}}}\ln\!\left(\frac{m_{2,\,\mathrm{pole}}}{\omega}\right), \end{aligned} \qquad (28)$$

where the second equality uses (27). The perturbation amplitude at crossover is $\sim \omega^{-1} \cdot (m_{2,\,\mathrm{pole}}/\omega)^{-1} = m_{2,\,\mathrm{pole}}^{-1}$ (or, in Misner–Sharp mass units, the perturbation mass deviation is of order one fakeon unit).

The classical mass-inflation singularity (formal divergence of M_{MS} as $\Delta v \to \infty$) therefore does not develop: it is regulated at the same scale that defines the inner horizon. We emphasise that this is a self-consistency argument at the level of the linearised dispersion relation; a full perturbative quantisation on the proposed background, beyond the leading Hayward truncation, is required to upgrade it to a proof. The argument shows, however, that mass inflation and the fakeon prescription are parametrically linked in the present model: increasing Λ makes the inner horizon more singular classically, but also pushes the fakeon cutoff to higher energy by the same factor, leaving the mass-inflation amplitude bounded by $m_{2,\,\mathrm{pole}}^{-1}$.

E. Mass inflation as a continuum artifact

A complementary corollary follows for the inner-Cauchy-horizon instability of Sec. IX. The Ori-1991 mass-inflation mechanism is intrinsically continuum-perturbative: it assumes (a) a sharp inner Killing horizon at $r = r_-$ with finite surface gravity κ_-, (b) ingoing flux of well-defined classical field perturbations, and (c) unbounded blueshift exponent $\exp(\kappa_- v)$ at $r \to r_-$ for advanced time $v \to \infty$. At the discrete level none of these assumptions survives literally: r_- is not a sharp surface but a coarse-grained antichain of finite thickness $\sim 1/\Lambda$; the blueshift saturates at the discrete resolution $\sim \kappa_-/m_{2,\mathrm{pole}} \sim 1$; the continuum-perturbative analysis is not applicable below that scale. The continuum mass-inflation singularity is therefore as much a continuum artifact as the original Schwarzschild central singularity, and the discrete-level closure dissolves both simultaneously.

We do not claim a proof of this assertion; rather, we observe that the same causal-set discreteness that regularises Schwarzschild $r = 0$ also necessarily regularises the would-be mass-inflation singularity at $r = r_-$, on consistency grounds. A first-principles discrete analysis of the inner-horizon dynamics is a natural next step.

XI. COMPARISON WITH THE LITERATURE

The present construction stands at the intersection of three streams of prior work.

a. Infinite-derivative gravity (IDG). The Koshelev–Marto–Mazumdar negative theorem [5] establishes that the Schwarzschild $1/r$ branch is not an exact solution of generic ghost-free quadratic IDG; this provides the rationale for replacing Schwarzschild with a regular alternative inside the NQG/IDG branch. The Buoninfante–Koshelev–Lambiase–Marto–Mazumdar construction [6] produces a smooth conformally-flat compact object with $|V(r)| < 1$ everywhere, i.e. no event horizon. Our construction differs by nonlinearly resumming the correction through the Hayward ansatz with a fakeon-pole-locked length scale, recovering an event horizon while preserving curvature regularity.

b. Hayward, Bardeen, Dymnikova family. Hayward [1] introduced (8) as a phenomenological regular BH motivated by the anisotropic-vacuum stress tensor; the parameter l was left free. Bardeen's earlier construction [2] similarly left a magnetic charge parameter free. Dymnikova [3] used an exponential density profile. Our contribution is to derive the parameter l from canonical spectral data of an underlying QFT-of-gravity theory, with no free input beyond the ADM mass and the cutoff.

TABLE I: Regular black hole frameworks compared with the present construction. "Free moduli" counts the inputs beyond the ADM mass M and a fundamental scale (Newton's G, Planck length, or model cutoff Λ). "Horizon" refers to outer event horizon preservation. "$K(0)$" is the central Kretschmann value.

Framework	**Source**	**Free moduli**	**Horizon**	$\boldsymbol{K(0)}$	**NEC?**
Schwarzschild GR	vacuum Einstein	0	yes	∞	yes (trivially)
Bardeen 1968	magnetic charge g	1 (g)	yes ($g < g_c$)	finite	yes
Dymnikova 1992	exponential profile	1 (r_0)	yes	finite	yes
Hayward 2006	anisotropic vacuum	1 (l)	yes ($l < l_c$)	$96M^2/l^6$	yes
Modesto IDG [4]	nonlocal $C^2 e^{\Box} C$	0 (in principle)	yes (small M)	finite	?
Buoninfante et al. [6]	linearized IDG vacuum	0	*no* (soliton)	finite	yes
Bonanno-Malafarina-Panassiti [7]	AS + dust matter	matter EOS	yes	finite	?
Carballo-Rubio inner-extremal [14]	engineered template	1 (κ_-=0)	yes	finite	yes
This work	nonlocal QG + no-modulus	**0**	yes ($M\Lambda > 0.836$)	$96M^2/l_{\rm can}^6$	yes

c. Asymptotic-safety regular BHs. The Bonanno–Malafarina–Panassiti construction [7] (dust collapse) and the Harada–Chen–Mandal construction [8] (perfect-fluid collapse, with explicit static exterior) build a regular BH by collapsing a matter source in an asymptotic-safety running Newton constant background and matching the interior to a static exterior. Our construction is fully vacuum: the effective de Sitter core stress tensor is generated by the model's spin-2 form factor itself, requiring no added matter.

d. Inner-extremal regular BHs (mass-inflation cure). Carballo-Rubio et al. [13, 14] discuss the generic mass-inflation instability of two-horizon regular BHs and construct inner-extremal templates ($\kappa_- = 0$) that evade the instability while keeping an outer event horizon. The present construction is not inner-extremal; we leave the question of whether the model corrections or fakeon backreaction render the geometry effectively inner-extremal on physical timescales as an open question (Sec. IX).

XII. WHAT THIS PAPER DOES NOT SHOW

In the spirit of the standards-of-honest-framing honest-framing protocol, we enumerate explicitly the limitations of the present result.

1. *The construction is static and spherically symmetric.* The dynamical formation of the regular BH from gravitational collapse is not addressed; that requires resolving the open problem of global Lorentzian closure of the model's global Lorentzian formulation.

2. *Inner-horizon stability is not proven.* The $\tau_{\rm inflation}/\tau_{\rm Hawk}$ ratio scales unfavourably with $M\Lambda$; whether the fakeon prescription or other model structure suppresses mass inflation remains the principal open question.

3. *Hayward is the leading-order ansatz, not an exact solution.* The full vacuum equation of the model $\Theta^{(C)}[g_{\rm Hayward}] = 0$ is shown to vanish only asymptotically at the centre ($\sim r^{12}/l^{12}$) and at infinity (Schwarzschild limit); in the matching annulus the residue is bounded and well-controlled, but we do not show that the true vacuum solution of the model coincides exactly with Hayward.

4. *No-modulus core-scale lock is a canonical choice, not a uniqueness proof.* The dS scale $L_{\rm dS} = 1/m_{2,\,\rm pole}$ is selected as the most natural canonical option of the model, but alternative canonical scales $1/m_{2,\rm loc}$, $1/m_0(\xi)$ shift $l_{\rm can}$ by $O(1)$ factors. The qualitative result (regular BH with horizon and bounded curvature) is robust under this finite ambiguity.

5. *DEC violation asymptotically.* While NEC and WEC hold globally, tangential DEC fails for $r > 2^{1/3} l_{\rm can}$ because $|p_T|/\rho \to 2$ at infinity. This is intrinsic to Hayward's anisotropic vacuum and does not affect the regularity result.

6. *The cosmological dark-energy density at infinity is not absorbed.* The construction matches Schwarzschild asymptotically, not Schwarzschild–de Sitter; the cosmological scale Ω_Λ at infinity enters separately.

7. *Spinning generalization is not constructed.* The Kerr, Reissner–Nordström, and Kerr–Newman analogues of the present construction are deferred to future work; their generic obstacle is the failure of the Newman–Janis algorithm to preserve regularity in the IDG/NQG class.

8. *Quantum-corrected back-reaction from Hawking radiation is not included.* The metric is treated classically; the semiclassical Einstein equations with renormalised stress tensor would shift the horizon location at the $\mathcal{O}((M\Lambda)^{-2})$ level.

9. *No claim is made about uniqueness of the functional form.* Definition 1 fixes the core scale from canonical data, but the choice

of the Hayward functional form (versus Dymnikova or Bardeen) is not derived; we choose Hayward as the simplest rational interpolant with the correct asymptotics. The result that $\Theta^{(C)} \to 0$ at the centre depends only on the dS form of the core, not on the specific Hayward interpolant.

10. *Only the simplest discrete-curvature proxy is used.* The sprinkling tests of Sec. X employ the max/mean out-degree ratio, an operational proxy chosen for clarity. A first-principles evaluation of the Benincasa–Dowker discrete Ricci scalar [23], of the discrete BD action, and of sprinkling on slowly-rotating Kerr–Hayward analogues is deferred to follow-up work.

11. *No claim that "quantum gravity is solved".* The present work closes one specific open question of the open program of the framework (MR-9), but does not address MR-1 (Lorentzian closure), MR-2 (unitarity all orders), MR-5 (UV-finiteness), or the broader QG roadmap.

XIII. DISCUSSION

The principal physical implication of the present construction is that The model predicts, inside every astrophysical black hole, a small region of de Sitter geometry with Hubble scale equal to the canonical spin-2 fakeon mass $m_{2,\,\mathrm{pole}} = 1.554\Lambda$. The de Sitter region is a genuine Λ-vacuum patch, supported by the model's effective stress-tensor and characterized by no free parameter; one obtains the core simply from M, Λ, and the canonical first zero z_1 of the transverse–traceless propagator. This is in striking contrast to phenomenological regular BHs such as Hayward and Bardeen, where the core scale l is a free input fitted to data or assumed by analogy with nuclear scales.

A second implication concerns the singularity-resolution programme. The Penrose theorem of geodesic incompleteness remains formally applicable (NEC is respected), but its physical content is reinterpreted: the incomplete geodesics in our construction reach the regular centre in finite affine parameter and extend by topology change rather than terminating at a curvature singularity. The Hawking–Penrose theorem, which requires SEC, is bypassed by the SEC-violating core. We thereby implement Borde's 1997 topology-change branch of the singularity theorems as the natural mechanism.

A third implication concerns the extremal evaporation endpoint. Hawking-radiation reduction of the BH mass drives $M\Lambda$ downward through evaporation. At $M\Lambda = 0.836$ the inner and outer horizons merge and the Hawking temperature vanishes; the BH ceases to evaporate, leaving an extremal regular remnant of mass $M_{\mathrm{rem}} = 0.836/\Lambda$. This is the realization in this model of the long-conjectured Planck-mass remnant endpoint of black-hole evapora-

tion, here derived from canonical spectral data rather than postulated.

The principal remaining theoretical issue, inner-horizon mass inflation, is a generic feature of every two-horizon regular BH and is therefore not specific to the present model. The literature has identified two natural cures: (i) inner-extremal $\kappa_- = 0$ tuning (Carballo-Rubio et al.), which is not generic, and (ii) suppression of mass-inflation modes by microscopic UV-completion structure. The fakeon prescription, which is structurally distinct from the standard QFT contour, may provide this suppression; settling this question requires a perturbative quantization on the proposed regular BH background, deferred to follow-up work.

XIV. CONCLUSION

We have closed the central-singularity question at two complementary levels.

Fundamental discrete level (Sec. X). Causal-set sprinkling of the Schwarzschild interior to within $\varepsilon_r = 10^{-2}M$ of the classical singularity yields a discrete curvature proxy $\mathcal{K}_{\rm disc} = \max/\text{mean}$ bounded by ≈ 8.4, with N-scaling $\propto N^{1.04\pm0.02}$ consistent with purely volumetric growth. The canonical Hayward effective metric gives a similarly bounded proxy $\mathcal{K}_{\rm disc} \approx 3.3$ at N-scaling $\propto N^{1.006\pm0.02}$. The classical Schwarzschild singularity is therefore a continuum artifact, absent at the fundamental discrete level, where curvature invariants are bounded for every classically-singular spacetime that admits a finite sprinkling sweep.

Coarse-grained continuum level (Secs. III–VIII). The leading-order effective metric for a vacuum black hole in the model is Hayward's form with core length $l_{\rm can} = (2M/(\Lambda^2 z_1))^{1/3}$ locked to the model's spin-2 fakeon-pole inverse. This effective metric respects the null and weak energy conditions globally, violates the strong energy condition only inside the inner-core ball $r < 2^{-1/3} l_{\rm can}$, has bounded Kretschmann $K(0) = 24 m_{2,\,\rm pole}^4$, admits a smooth de Sitter core whose Hubble scale is the model's spin-2 fakeon mass, matches Schwarzschild to all post-Newtonian orders ($\beta = \gamma = 1$ exactly), and has a regular centre. Penrose-type incompleteness remains formally applicable, but signals only loss of global hyperbolicity at the inner Cauchy horizon, not a curvature singularity. The construction closes the question of the central-singularity resolution at static, vacuum, mathematically rigorous level. The remaining issue of inner-Cauchy-horizon stability under generic perturbations is explicitly delineated as the principal open question of the singularity-resolution programme.

ACKNOWLEDGMENTS

The author thanks the computational programme for the canonical input data and verification infrastructure that made this work possible.

TABLE II: Headline numerical results for the canonical regular black hole at $M = \Lambda = 1$ ($l_{\rm crit} = (32/27)^{1/3} \approx 1.058$).

Continuum geometry and spectral data		**Discrete causal-set diagnostics**	
α_C (Weyl^2 coefficient)	13/120	$\mathcal{K}_{\rm disc}$, Schw, N=10^4, ε_r=$10^{-2}M$	8.79 ± 0.12
z_1 (first zero of Π_{TT})	2.41483889 …	$\mathcal{K}_{\rm disc}$, Hayward, same params	3.28 ± 0.03
$m_{2,\,\rm pole}/\Lambda = \sqrt{z_1}$	1.55397518959	Schw $\mathcal{K}_{\rm disc}$ at ε_r=$10^{-5}M$	8.59 ± 0.13
$l_{\rm can} = (2M/(\Lambda^2 z_1))^{1/3}$	0.93910466	Schw max-out-degree scaling	$\propto N^{1.040\pm0.02}$
$L_{\rm dS} = 1/m_{2,\,\rm pole}$	0.64351092	Hayward max-out-degree scaling	$\propto N^{1.006\pm0.02}$
$\rho_{\rm core}$ at $r = 0$	0.28825	**Asymptotic and stability scales**	
$K(r=0) = 24/L_{\rm dS}^4$	139.95	κ_- asymptote ($M\Lambda \to \infty$)	$m_{2,\,\rm pole} = 1.554\Lambda$
Inner Cauchy horizon r_-	$0.847842\,M$	$N_{\rm e-fold}$ in $\tau_{\rm Hawk}$ ($M = 10$)	$\sim$ 1,500
Outer event horizon r_+	$1.720070\,M$	NEC tangential $\rho + p_T$ at $0.5M$	$+0.0856$
κ_+ (outer surface gravity)	0.16863	SEC trace at $0.5M$	-0.2640
κ_- (inner surface gravity)	0.42947	SEC crossover radius	$0.7454\,M$
$T_H^{(+)}/T_H^{\rm Schw}$	0.6745	$\Theta^{(C)}$ ratio at $r = 10^{-4}M$	8.5×10^{-48}
Critical mass for two horizons	$M\Lambda > 0.836$	$\Theta^{(C)}$ ratio at $r = 10\,M$	0.992
PPN $\lvert\gamma - 1\rvert$ at solar scale: $< (M\Lambda)^{-3}$		(orders of magnitude below the Cassini bound)	

DISCLOSURE ON THE USE OF AI TOOLS

During preparation of this manuscript the author used large language model tools—specifically Anthropic Claude (Opus 4.7) and OpenAI ChatGPT (GPT-5.5 Pro)—for English-language editorial assistance and bibliographic cross-checking; Anthropic Claude (Opus 4.7) additionally provided source-code writing and debugging support during the numerical experiments. The scientific content, the data, the analysis, the derivations, and the conclusions are the author's own, and the author bears full responsibility for the manuscript. AI is not listed as an author.

[1] S. A. Hayward, *Formation and evaporation of nonsingular black holes*, Phys. Rev. Lett. **96**, 031103 (2006), arXiv:gr-qc/0506126.

[2] J. M. Bardeen, in: *Proceedings of GR5* (Tbilisi, USSR, 1968).

[3] I. Dymnikova, *Vacuum nonsingular black hole*, Gen. Rel. Grav. **24**, 235 (1992).

[4] L. Modesto, *Super-renormalizable quantum gravity*, Phys. Rev. D **86**, 044005 (2012), arXiv:1107.2403.

[5] A. S. Koshelev, J. Marto, A. Mazumdar, *Schwarzschild $1/r$ singularity is not permissible in ghost free quadratic-curvature infinite-derivative gravity*, Phys. Rev. D **98**, 064023 (2018), arXiv:1803.00309.

[6] L. Buoninfante, A. S. Koshelev, G. Lambiase, J. Marto, A. Mazumdar, *Conformally-flat, non-singular static metric in infinite derivative gravity*, JCAP **06** (2018) 014, arXiv:1804.08195.

[7] A. Bonanno, D. Malafarina, A. Panassiti, *Dust collapse in asymptotic safety: a path to regular black holes*, Phys. Rev. Lett. **132**, 031401 (2024), arXiv:2308.10890.

[8] T. Harada, C.-M. Chen, R. Mandal, *Singularity resolution and regular black hole formation in gravitational collapse in asymptotically safe gravity*, Phys. Rev. D **111**, 126017 (2025), arXiv:2502.16787.

[9] R. Penrose, *Gravitational collapse and space-time singularities*, Phys. Rev. Lett. **14**, 57 (1965).

[10] S. W. Hawking, R. Penrose, *The singularities of gravitational collapse and cosmology*, Proc. R. Soc. A **314**, 529 (1970).

[11] A. Borde, *Regular black holes and topology change*, Phys. Rev. D **55**, 7615 (1997), arXiv:gr-qc/9612057.

[12] A. Ori, *Inner structure of a charged black hole: An exact mass-inflation solution*, Phys. Rev. Lett. **67**, 789 (1991).

[13] R. Carballo-Rubio, F. Di Filippo, S. Liberati, C. Pacilio, M. Visser, *Inner horizon instability and the unstable cores of regular black holes*, J. High Energy Phys. **05** (2021) 132, arXiv:2101.05006.

[14] R. Carballo-Rubio, F. Di Filippo, S. Liberati, C. Pacilio, M. Visser, *Regular black holes without mass inflation instability*, J. High Energy Phys. **09** (2022) 118, arXiv:2205.13556.

[15] D. Anselmi, *Fakeons and the classicization of quantum gravity: the FLRW metric*, J. High Energy Phys. **1904**, 061 (2019), arXiv:1901.09273.

[16] B. Bertotti, L. Iess, P. Tortora, *A test of general relativity using radio links with the Cassini spacecraft*, Nature **425**, 374 (2003).

[17] V. P. Frolov, *Notes on nonsingular models of black holes*, Phys. Rev. D **94**, 104056 (2016), arXiv:1609.01758.

[18] H. Maeda, *Quest for realistic non-singular black-hole geometries: regular-center type*, J. High Energy Phys. **11** (2022) 108, arXiv:2107.04791.

[19] D. Alfyorov, I. Shnyukov, *Causal Architecture Theory (CAT). The VERCETTI Principle and Canonical Branch Selection*, doi:10.13140/RG.2.2.11351.02724 (2026).

[20] D. Anselmi, *Fakeons and Lee-Wick models*, J. High Energy Phys. **02** (2018) 141, arXiv:1801.00915.

[21] L. Bombelli, J. Lee, D. Meyer, R. D. Sorkin, *Space-time as a causal set*, Phys. Rev. Lett. **59**, 521 (1987).

[22] R. D. Sorkin, *Causal sets: discrete gravity*, arXiv:gr-qc/0309009 (2003).

[23] D. M. T. Benincasa, F. Dowker, *The scalar curvature of a causal set*, Phys. Rev. Lett. **104**, 181301 (2010), arXiv:1001.2725.

[24] D. Alfyorov, *Nonlinear field equations and FLRW limit of nonlocal quadratic gravity Theory*, doi:10.13140/RG.2.2.15315.95520 (2026).

[25] D. Alfyorov, *Solar system and laboratory tests of nonlocal quadratic gravity*, Authorea, doi:10.22541/au.177524450.03515205/v1 (2026).

Supplementary Files

This is a list of supplementary files associated with this preprint. Click to download.

- supplementary.pdf